

# Analysis of GNSS MBOC Pilot and Data Signal Joint Tracking

Xue Wang<sup>1,2,3</sup>, Zhenghong Zhu<sup>4,\*</sup>, Yao Guo<sup>1,3</sup>, Xiaochun Lu<sup>1,2</sup>

1. National Time Service Center, Chinese Academy of Science, Xi'an, Shaanxi, 710600, China

2. Key Laboratory of Precision Navigation, Positioning and Timing Technology, Chinese Academy of Sciences, Xi'an, Shaanxi, 710600, China

3. School of Electronic and Communication Engineering, University of Chinese Academy of Sciences, Beijing, 101408

4. Department of Mechanical Engineering, York University, M3J 1P3, Canada

Xue Wang, Email: [wangxue@ntsc.ac.cn](mailto:wangxue@ntsc.ac.cn) Tel: +1 437 9985869 /+86 18066555869

\* Corresponding Author: Zhenghong Zhu, Email: [gzh@yorku.ca](mailto:gzh@yorku.ca) Tel: (416) 7362100 x 77729

Abstract

With the launched of the new generation GPS satellite, the modern signal L1C began to broadcast. At present, BDS, GPS, GALILEO all broadcast the new civil signal MBOC at 1575.42MHz. The MBOC signal uses a modulation method in which the pilot and the data signals are separated and constant envelope multiplexing with other authorized signals. However, these modulation methods have evolved a variety of joint receiving algorithms. In the GNSS receiver COSTAS loop tracking process, the carrier phase and code phase are both simultaneously tracked by PLL and DLL. Therefore, in the joint tracking process, the high synchronization and stability of phase between pilot code and data code, and code-to-carrier phase are also required.

The paper introduces the optimal design strategy for MBOC signal joint tracking, in which the amplitude and phase output in COSTAS loop tracking processing is jointed in the loop phase discriminator and loop filter with the composite coefficients. According to the different modulations of each system, these composite coefficients are determined by the signals modulation phase relationship and power relationship. Through the BDS data verification, the advantages of joint tracking are demonstrated. The influences of signal coherencies in the joint tracking process are analyzed. The coherencies of between each signal code and code-to-carrier in GPS L1C, BDS B1C, and GALILEO E1C signals are evaluated by high Carrier-to-Noise ratio signal, which is acquired with the National Time Service Center CAS 40-meter antenna Signal in Space Quality Assessment System. The results verify the GNSS signal in space meets joint tracking requirements, and the joint tracking method has practical application value.

*Keywords: GNSS MBOC signal, joint tracking, codes phase coherency, code-to-carrier phase coherency, Signal in Space Quality Assessment*

## INTRODUCTION

In the decades, four main GNSS systems (GPS, BDS, GLONASS, and GALILEO), as well as some regional systems, such as QZSS and IRNSS, will broadcast many update signals in different frequencies. BDS, GPS, and GALILEO all designed the new civil MBOC signal at 1575.42MHz. With the new GPS satellite launched, the GPS modern signal L1C began to broadcast. At present, all MBOC modulation signals are broadcasted.

The MBOC signal uses a modulation method in which the pilot and the data components are separated and constant envelope multiplexing with other civil and military signals. Similar to the Composite Binary Offset Carrier (CBOC) and Time Multiplexed BOC (TMBOC) modulations employ respectively by Galileo E1, GPS L1C, and QZSS L1C, the BDS B1C adopts Quadrature Multiplexed BOC (QMBOC) modulation [1, 2, 3]. In the near future, new processing methods for new signals are emerging [4, 5].

Tracking loops (COSTAS) are the core of GNSS signal receiver, including Delay Locked Loops (DLL) and Phase Locked Loops (PLL). Synchronism with the spreading code is kept by DLL typically aided by the carrier tracking. Phase Locked Loops (PLL) has been an almost universal solution for carrier tracking. These are the loops that have to cope with signal dynamics caused by transmitter and receiver movement [6]. A common feature of MBOC is the new modulation schemes with data and pilot components. The various joint tracking modes are designed.

The outputs of pilot and data components are calculated after correlator or phase discriminator with the composite coefficients, the tracking performance is better than a single signal. But the approach suffers from  $C/N_0$ , code coherency and code-to-carrier coherency encountered in phase-locked loops. The high enough signal to noise ratio is important to get accurate estimates of the signal received phase and frequency provided. The results verify the GNSS signal in space meets joint tracking requirements, with high carrier-to-noise ratio signal data, which are collected with the National Time Service Center CAS 40-meter antenna Signal in Space Quality Assessment System.

The paper introduces the MBOC signal and receiver construction. The joint tracking is described, and then the BDS QMBOC signal joint tracking results are shown. The effects to joint tracking, by  $C/N_0$ , codes coherency and code-to-carrier

coherency are analyzed. Finally, the coherency of each code and code-to-carrier coherency in BDS B1C, are evaluated by high carrier-to-noise ratio signal.

## 1. The Signal Modulation and Receiver Construction

### 1.1 BDS B1C signal

BDS B1C signal consists of pilot signals  $S_{B1Cpa}$  and  $S_{B1Cpb}$ , a data signal  $S_{B1Cd}$ , The power relation between the data component and the pilot component is 1:3, and the pilot signal  $S_{B1Cp}$  includes  $S_{B1Cpa}$  and  $S_{B1Cpb}$ . These are shown in table 1[3].

Table 1 BDS B1C signal

Signal	Channel	Modulation	Phase	Power Ratio	
B1C	$S_{B1Cd}$	BOC(1,1)	0	11/44	
	$S_{B1Cp}$	$S_{B1Cpa}$	BOC(1,1)	90	29/44
		$S_{B1Cpb}$	BOC(6,1)	0	4/44

The expression of the B1C Baseband signal is as the follows.

$$\begin{aligned}
 S_{B1C}(t) = & \frac{1}{2} S_{B1Cd} + j \frac{\sqrt{3}}{2} S_{B1Cp} = \sqrt{\frac{11}{44}} D_{B1Cd} \cdot C_{B1Cd} \cdot \text{sign}(\sin(2\pi f_{SCB1Cd} t)) \\
 & + \sqrt{\frac{4}{44}} C_{B1Cp} \cdot \text{sign}(\sin(2\pi f_{SCB1Cpb} t)) \\
 & + j \sqrt{\frac{29}{44}} C_{B1Cp} \cdot \text{sign}(\sin(2\pi f_{SCB1Cpa} t))
 \end{aligned} \quad (1)$$

Where  $f_{SCB1Cd}=1.023MHz$ ,  $f_{SCB1Cpa}=1.023MHz$ ,  $f_{SCB1Cpb}=6.138MHz$ , in Eq.1, the pilot component consists of BOC(1,1) and BOC(6,1), are called Quadrature Multiplexed BOC (QMBOC(6,1,4/33)). And its baseband signal repression is shown as follow.

$$S_{QMBOC}(t) = \sqrt{\frac{29}{33}} S_{BOC(1,1)}(t) - j \sqrt{\frac{4}{33}} S_{BOC(6,1)}(t) \quad (2)$$

The BOC(1,1) and BOC(6,1) are respectively modulated on two orthogonal carriers. The waveform of QMBOC(6,1,4/33) is shown in fig.1.

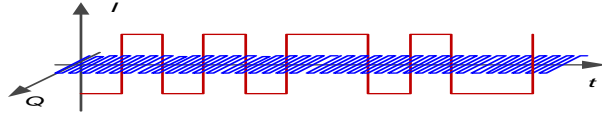


Figure 1 the waveform of QMBOC(6,1,4/33)

Baseband signal autocorrelation function is in Eq.3:

$$R_{QMBOC}(\tau) = E\{S_{QMBOC}(t)S_{QMBOC}^*(t)\} = \sqrt{\frac{29}{33}}R_{BOC(1,1)}(\tau) + \sqrt{\frac{4}{33}}R_{BOC(6,1)}(\tau) \quad (3)$$

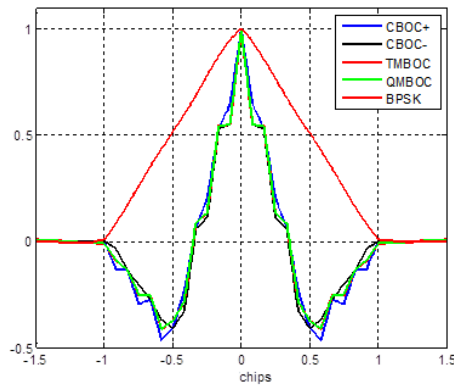


Fig.2 the autocorrelation Curves of QMBOC, TMBOC, CBOC-, CBOC+, and BPSK

Compared to TMBOC and CBOC, because of the quadrature phase, the components of BOC(1,1) and BOC(6,1) in BDS QMBOC are less internal interference in correlation processing.

## 2、GNSS signal receive processing

### 2.1 Basic BOC signal tracking loops

In fig.3, the BOC modulation tracking loop is shown. BOC signal tracking is achieved by delaying the input signal, selecting the appropriate integration window and loop parameters. Where K is the duration of the subcarrier in samples, and L defines the total number of samples available for loop parameter estimation. It is important to note that the squaring operation is a complex squaring and not the squared magnitude.

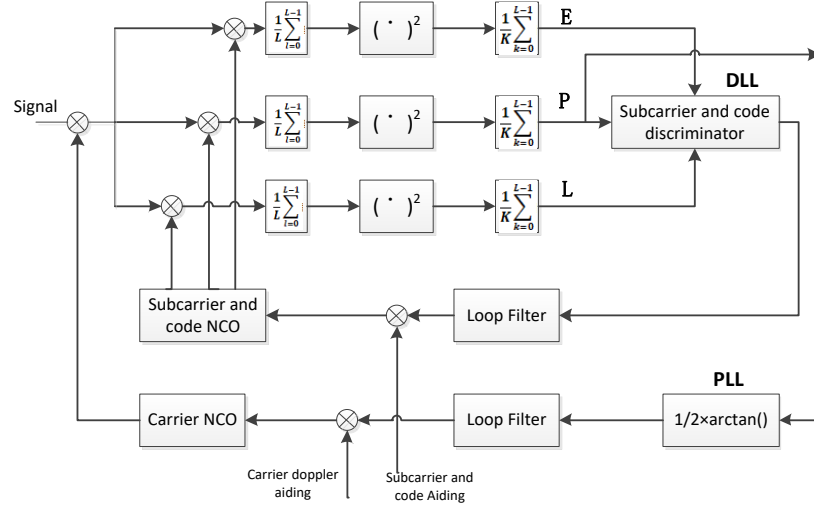


Fig.3 tracking of GNSS signals adopting a BOC modulation

Eq. 4 provides navigation signal processing mathematical description.

$$\begin{aligned}
 IE &= A \cdot D \cdot \sin(\pi \delta_f T) \cdot \cos(\delta_\varphi) \cdot R(\delta_\tau + \frac{d}{2}) + n_{IE} \\
 IP &= A \cdot D \cdot \sin(\pi \delta_f T) \cdot \cos(\delta_\varphi) \cdot R(\delta_\tau) + n_{IP} \\
 IL &= A \cdot D \cdot \sin(\pi \delta_f T) \cdot \cos(\delta_\varphi) \cdot R(\delta_\tau - \frac{d}{2}) + n_{IL} \\
 QE &= A \cdot D \cdot \sin(\pi \delta_f T) \cdot \sin(\delta_\varphi) \cdot R(\delta_\tau + \frac{d}{2}) + n_{QE} \\
 QP &= A \cdot D \cdot \sin(\pi \delta_f T) \cdot \sin(\delta_\varphi) \cdot R(\delta_\tau) + n_{QP} \\
 QL &= A \cdot D \cdot \sin(\pi \delta_f T) \cdot \sin(\delta_\varphi) \cdot R(\delta_\tau - \frac{d}{2}) + n_{QL}
 \end{aligned} \tag{4}$$

Where  $A$  is the signal amplitude,  $D$  is the message,  $\delta_f$  is the frequency bias between the local signal and receive signal,  $T$  is the Integration Time.  $\delta_\tau$  is the code phase bias between local signal and receive signal,  $\delta_\varphi$  is the carrier phase tracking error[7].

The carrier phase error is gotten by calculating with  $I_p$ 、 $Q_p$  in the Loop tracking carrier phase discriminator, goes through a PLL loop filter and becomes the input parameters to control carrier numerically controlled oscillator(NCO).

The code phase error is gotten by calculating with  $I_E$ 、 $I_L$ 、 $Q_E$ 、 $Q_L$  in the Loop tracking code phase discriminator, goes through DLL filter and becomes the input parameters to control code numerically controlled oscillator(NCO). The Code NCO and Carrier NCO output the frequency of local code and carrier.

## 2.2 Joint tracking loops

The  $S_{B1Cd}$  and  $S_{B1Cpa}$  signals are used to simulate joint tracking, their modulation is BOC(1,1). The each signal discriminator outputs are linear joint by the different coefficient, the weight coefficient of the data component is  $\alpha$ , and the pilot component is  $\beta$ . The values of  $\alpha$  and  $\beta$  are corresponding to the power ratio. According to Eq.1,  $P_{B1Cd} : P_{B1Cpa} = 11:29$ , so  $\alpha = 11$ ,  $\beta = 29$ . The joint Tracking loop is shown in fig 4[8].

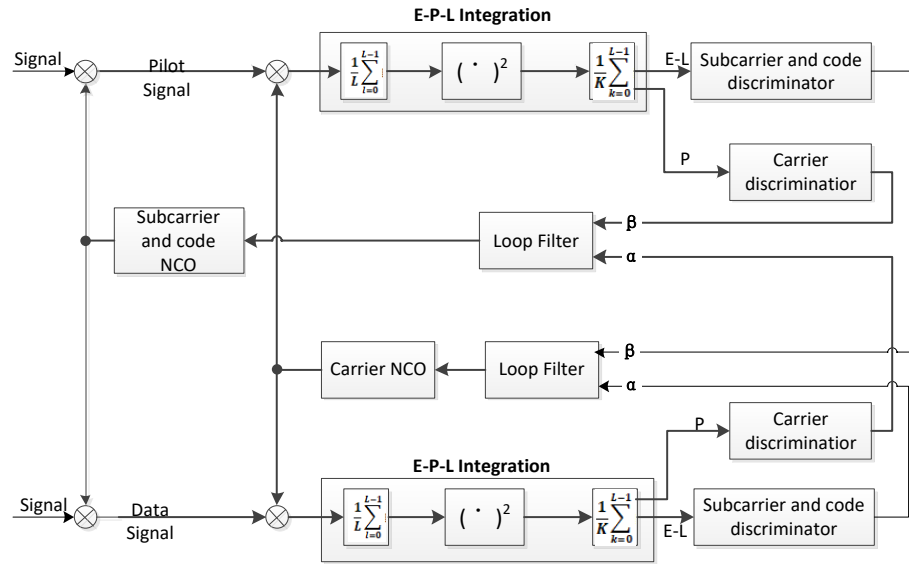


Figure 4 Discriminator output linear combined structure

In the case of joint Tracking, the new discriminator error of PLL and DLL is as follow.

$$\Delta \hat{\tau}_{cmb}(t) = \frac{11}{40} \Delta \hat{\tau}_d(t) + \frac{29}{40} \Delta \hat{\tau}_p(t) \quad (5)$$

$$\Delta \hat{\varphi}_{cmb}(t) = \frac{11}{40} \Delta \hat{\varphi}_d(t) + \frac{29}{40} \Delta \hat{\varphi}_p(t) \quad (6)$$

where  $\hat{\Delta\tau}_d$  and  $\hat{\Delta\tau}_p$  represent the code discriminator error of data and pilot component.  $\hat{\Delta\phi}_d$  and  $\hat{\Delta\phi}_p$  represent the carrier discriminator error.  $\hat{\Delta\tau}_{cmb}$  and  $\hat{\Delta\phi}_{cmb}$  are respectively the joint discriminator error.

Because of no data Bit in the pilot component, the ATan2 discriminator methods are chosen in PLL, and Its effective range is  $(-\pi, \pi)$ . The ATan discriminator method is used in PLL of data component, and Its effective range is  $(-\pi/2, \pi/2)$ . So the tracking threshold of the pilot component is lower than the data component. The relationship of the carrier between pilot and data must pay attention to the phase relation,  $P_p = (IP_p + jQP_p)e^{(-j\pi/2)}$ .

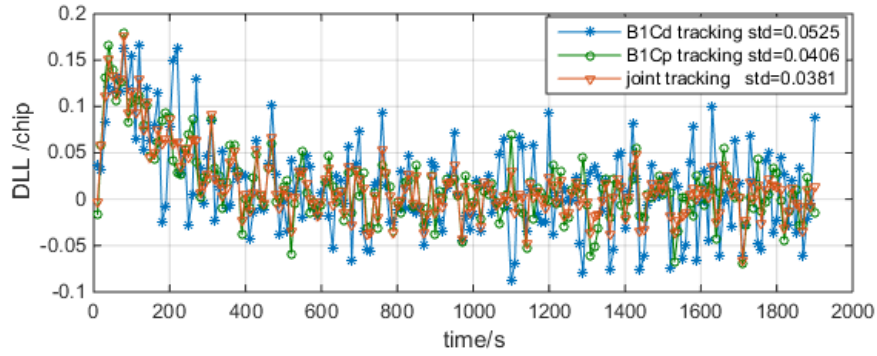


Figure 5 Comparison of DLL discriminator output

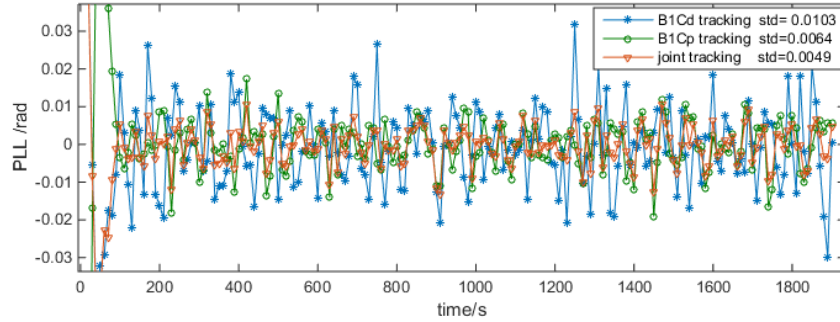


Figure 6 Comparison of PLL discriminator output

According to the simulation with Eq.5 and Eq.6, in the case of joint tracking methods, the phase and power relationship between data signal and pilot signal are very important, the parameters are defined as the power ratio, codes coherency and code-to-carrier coherency.

### 3 Performance parameters

#### 3.1 Power ratio

In the case of signal stably tracking, the receiver gets the available signal power, by the output of correlation integration IP in Eq.4. Therefore, the power ratio of each component signal to total power is calculated with receiving signal and local signal, as follows.

$$\eta(\tau) = \frac{\left( \int_0^{T_p} S_{re}(t) S_{i-local}(t-\tau) dt \right)^2}{\left( \int_0^{T_p} |S_{re}(t)|^2 dt \right)} \quad (7)$$

Where  $T_p$  is the integration time or the code period,  $\eta(0)$  is the power ratio.

Table 2 Each B1C signal power ratios in the BDS No.28 and No.30 satellite

	B1Cd	B1Cp	B1Cpa	B1Cpb	Design Ratio
BDSIII MEO PRN 30	10.7	33.0	29.4	3.6	11:33: 29: 4
BDSIII MEO PRN 28	11.0	33.0	29.4	3.6	

#### 3.2 Coherency parameters

If the code phase of joint tracking is different from  $S_{B1Cd}$  and  $S_{B1Cpa}$ , the correlation peak will decrease quickly following with the correlation curve. As shown in fig.6, The slope of the QMBOC curve is 5.4, and the BOC(1,1) is 3 in the  $-0.1 \sim +0.1$  chips. So the error of code phase is 0.1 chip, the amplitude of QMBOC correlation peak decreases 3dB, the power will decrease 6dB. This is a serious impact on signal tracking.

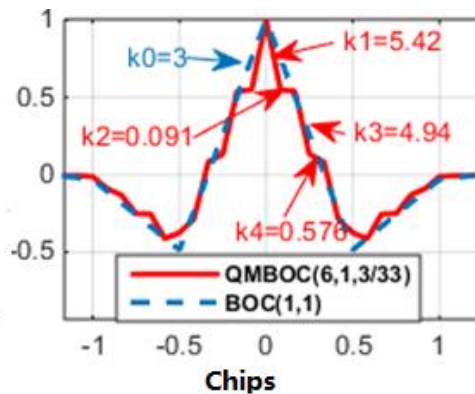


Fig.7 The correlation curve of QMBOC and BOC(1,1)



The fig.7 shows the correlation curves of QMBOC, and the slope of the curve in each chip step is different, and K1, K2, K3, and K4 are marked, k0 is the slope of BOC(1,1) autocorrelation curve.

The time difference between signals consists of the variable time difference and the average time difference. In BDS, the average time difference (ISCB1Cd) is broadcast in the B-CNAV1 message to compensate for the group delay differential between the B1C data component and the B1C pilot component [3]. The codes coherency and code-to-carrier coherency represent variable time difference. Using Carrier pseudorange and code pseudorange measured with the software receiver, the code coherency of the data component and pilot component is defined as follows.

$$\Delta\rho_{1, k} = \rho_1(T + t_k) - \rho_1(t_k) \quad (8)$$

$$\Delta\rho_{2, k} = \rho_2(T + t_k) - \rho_2(t_k) \quad (9)$$

$$CPD_k = \Delta\rho_{1, k} - \Delta\rho_{2, k} \quad (10)$$

Where T is the time steps,  $k=1,2,3, \dots$

$t_k$  is the time of  $k$  steps;

$\rho_i(t)$  represents the code pseudorange results of the  $i$ th signal at  $t_k$ ;

$\Delta\rho_{i,k}$  is the difference of code pseudorange between  $t_k$  and  $t_{k+T}$ .

$CPD_k$  is the code coherency of two signals of between  $t_k$  and  $t_{k+T}$ .

The code-carrier coherency is defined as follows.

$$\Delta\rho_k = \rho(T + t_k) - \rho(t_k) \quad (11)$$

$$\Delta\psi_k = \psi(T + t_k) - \psi(t_k) \quad (12)$$

$$CCD_k = \Delta\rho_k - \Delta\psi_k \quad (13)$$

Where T is the time steps,  $k=1,2,3, \dots$

$t_k$  is the time of  $k$  steps;

$\rho(t)$  represents the code pseudorange results of the  $i$ th signal at  $t_k$ ;

$\Delta\rho_{i,k}$  is the difference of code pseudorange between  $t_k$  and  $t_{k+T}$ .

$\psi(t)$  represents the carrier phase pseudorange results of the  $i$ th signal at  $t_k$ ;

$\Delta\psi_k$  is the difference of carrier phase pseudorange between  $t_k$  and  $t_{k+T}$ .

$CPD_k$  is the code coherency of two signals of between  $t_k$  and  $t_{k+T}$ .

## 4. GNSS signal in space quality assessment system

The GNSS Signal in Space Quality Assessment System was built by the National Time Service Center, the Chinese Academy of Sciences, in 2014. Fig.8 shows the structure of the high-gain signal receiving link, including antenna, RF channel, terminal, calibration, time-frequency reference, and data processing. The system maintains high-stability time-frequency performance through the cesium atomic clock. With the high sampling and low distortion acquisition equipment, acquisition data is achieved the best work conditions for accurately signal quality evaluation.

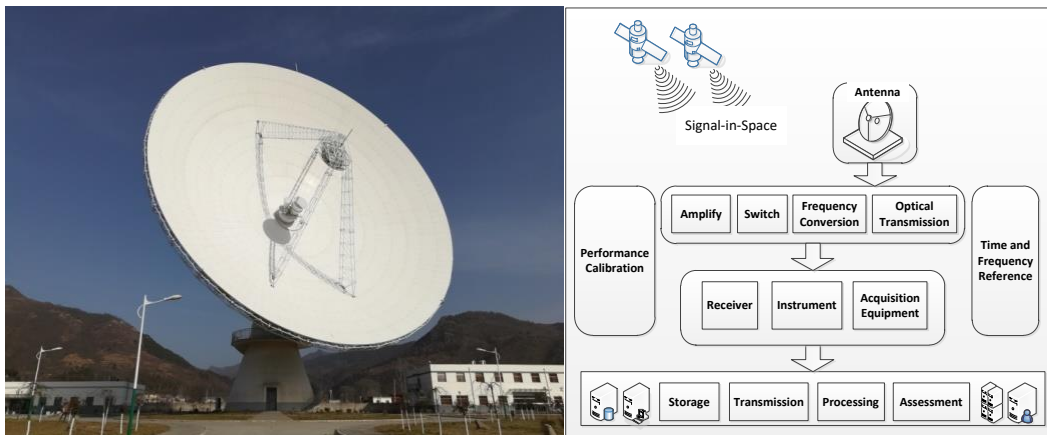


Fig. 8 40-meters antenna receiving system and High gain signal receiving link structure

As shown in Fig.8, the 40 meters main reflecting surface works in the L-band (1.10-1.75 GHz) and antenna gain 51.2 dBi@1.1 GHz.

## 5. Analysis results

The B1C signal data from NTSC the GNSS signal in space quality assessment system was collected, and its length is 9s. After acquirement and tracking, the Pseudorange of code and carrier phase are measured. With Eq.10 and Eq.13, the time difference between each code and carrier are calculated. The results are shown in fig.9 and fig.10, the statistics value of results in the Table3 and Table 4

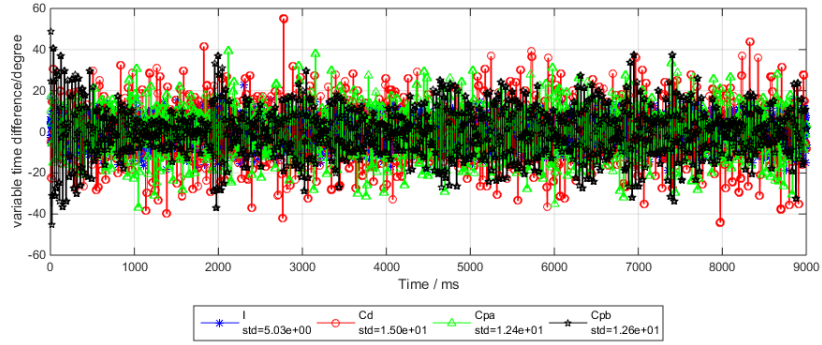


Fig.9 the variable time difference between codes and carrier (degree)

Table 3 the standard deviation of variation between code and carrier phase

Variable time difference	B1I	B1Cd	B1Cpa	B1Cpb
$\sigma$ (ns)	0.003	0.001	0.001	0.001

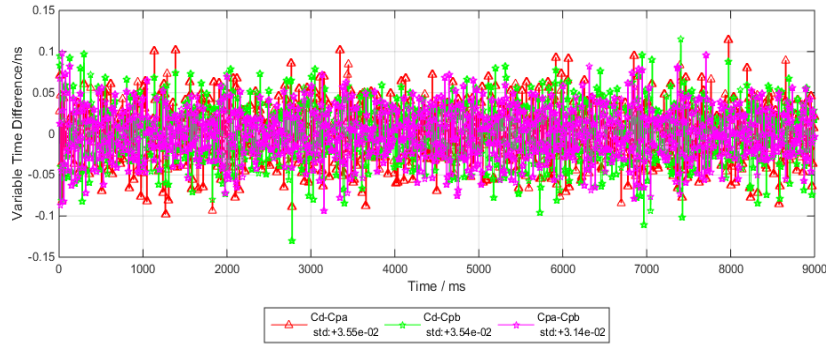


Fig.10 the variable time difference between codes

Table 4 the standard deviation of variation between code phase

Variable time difference	Cd-Cpa	Cd-Cpb	Cpa-Cpb
$\sigma$ (ns)	0.035	0.035	0.031

As shown in the Fig.9 and Fig.10, the variation between each code and carrier phase is good at meeting the requirement of joint tracking.

## 6、 Conclusion

The joint tracking method is described in this paper. The outputs of discriminator are linear joint by the different coefficient, and the weight coefficient of each component is detected by the signal power ratio. The phase and power relationship between data and pilot signal are very important parameters to affect joint tracking. The methods of the power ratio, code coherency and code-to-carrier coherency are analyzed. These parameters of BDS MBOC signal are evaluated with the National Time Service Center CAS 40-meter antenna Signal in

Space Quality Assessment System. The results verify the GNSS signal in space meets joint tracking requirements.

#### Reference

- [1] Global Positioning System Wing (GPSW) Systems Engineering & Integration, Interface Specification Is-GPS-800 Revision A.
- [2] European GNSS (Galileo) Open Service Signal In Space Interface Control Document.
- [3] China Satellite Navigation Office, "Interface Control Document for B1C and B2a (Beta version in Chinese)." August 2017.
- [4] Borio, Daniele, C. O'Driscoll, and G. Lachapelle. "Coherent, No coherent, and Differentially Coherent Combining Techniques for Acquisition of New Composite GNSS Signals." *IEEE Transactions on Aerospace & Electronic Systems* 45.3(2009): 1227-1240.
- [5] Yao, Z., M. Lu, and Z. M. Feng. "Quadrature multiplexed BOC modulation for interoperable GNSS signals." *Electronics Letters* 46.17(2010):1234-1236.
- [6] Seokho Yoon, Ickho Song, A DS-CDMA Code Acquisition Scheme Robust to Residual Code Phase Offset Variation. *IEEE TRANSACTIONS ON VEHICULAR TECHNOLOGY, VOL. 49, NO. 6, November 2000.*
- [7] Betz J W, Kolodziejki, KR. Generalized Theory of Code Tracking with an Early-Late Discriminator Part I: Lower Bound and Coherent Processing[J]. *IEEE Transactions on Aerospace & Electronics Systems*, 2009, 45(04):1538-1556.
- [8] Yafeng Li, Nagaraj C. Shivaramaiah. An open source BDS-3 B1C/B2a SDR receiver, *Proceedings of the 2018 International Technical Meeting, ION ITM 2018, Reston, Virginia, January 29-February 1, 2018.*